Dynamics of chaotic maps with global inhomogeneous coupling

EUROPHYSICS LETTERS 15 February 1999

Europhys. Lett., **45** (4), pp. 424-430 (1999)

Dynamics of chaotic maps with global inhomogeneous coupling

D. H. Zanette

Consejo Nacional de Investigaciones Científicas y Técnicas, Centro Atómico Bariloche and Instituto Balseiro - 8400 Bariloche, Río Negro, Argentina

(received 6 April 1998; accepted in final form 30 November 1998)

PACS. 05.20−y – Classical statistical mechanics.
PACS. 05.45+b – Theory and models of chaotic systems.
PACS. 87.10+e – General theory and mathematical aspects.

Abstract. – A population of globally coupled logistic maps with inhomogeneous coupling is numerically studied. It is shown that when the coupling intensities take large values with relatively small dispersion the system is entrained in fully synchronous motion. When synchronization is unstable, instead, a regime with complex correlation between the dynamics of each map and its coupling intensity is observed. Self-averaging of internal fluctuations holds in this system for small population sizes, whereas it breaks down when the population grows.

It has been pointed out that global interactions between active elements can play a leading role in governing the dynamics of a wide class of natural systems [1], that range from surface catalytic reactions [2] to neural networks [3] and biological populations [4]. This has recently motivated rather intensive investigation of globally coupled ensembles of dynamical systems. For instance, a widely studied form of global coupling between N identical discrete-time mappings whose individual dynamics is given by $\mathbf{x}(t+1) = \mathbf{F}[\mathbf{x}(t)]$ is [5]

$$\mathbf{x}_i(t+1) = (1-\epsilon)\mathbf{F}[\mathbf{x}_i(t)] + \frac{\epsilon}{N}\sum_{j=1}^{N}\mathbf{F}[\mathbf{x}_j(t)]\,, \tag{1}$$

where ϵ ($0 \leq \epsilon \leq 1$) measures the strength of coupling and $i = 1, 2, \ldots, N$ labels the elements in the ensemble. In this form of global coupling, as ϵ grows, the individual dynamics is gradually replaced by the global average $\langle \mathbf{F} \rangle = N^{-1}\sum_j \mathbf{F}(\mathbf{x}_j)$. For $\epsilon = 1$, the ensemble is fully synchronized after the first time step, and from then on all the elements have identical evolution. Full synchronization is in fact linearly stable for $\epsilon > 1 - \exp[-\lambda_{\max}]$, where $\lambda_{\max}$ is the maximum Lyapunov exponent of the mapping that defines the individual dynamics [6]. At lower values of the coupling intensity, partial synchronization —typically, in the form of clustering [5, 7]— can be observed.

From a realistic viewpoint, however, it is unlikely to find a globally coupled system whose elements are strictly identical. Some attention has therefore been paid to inhomogeneous

ensembles [1, 8], where the elements differ in the value of one or more parameters of their individual dynamics, which are distributed over prescribed probability densities. A different kind of inhomogeneity, that could plausibly appear in realistic models, would take into account that the coupling intensity is not the same for all the elements. It could be reasonable to suppose that, although still interacting through global averages, each element is affected with different strength by the ensemble. This should apply in particular to biological populations: the possibility of introducing inhomogeneities in coupling intensities has already been qualitatively discussed in connection with a sociological problem [9]. In this letter, the dynamics of an ensemble of N globally coupled logistic maps with inhomogeneous coupling intensities is studied. Consider the system of coupled mappings

$$x_i(t+1) = (1-\epsilon_i) f[x_i(t)] + \epsilon_i \langle f(t) \rangle, \qquad i = 1, \ldots, N\,, \tag{2}$$

with $f(x) = 4x(1-x)$ —which corresponds to the extreme chaotic regime of the logistic map— and $\langle f(t) \rangle = N^{-1} \sum_j f[x_j(t)]$. The coupling intensities ϵ_i are chosen at random from a probability distribution $P(\epsilon)$, with $0 \leq \epsilon \leq 1$. In [10], some preliminary results on system (2) have been presented for the case where ϵ is uniformly distributed between two given values. Here, instead, $P(\epsilon)$ is taken to be a truncated Gaussian function:

$$P(\epsilon) = \mathcal{N} \begin{cases} \exp[-(\epsilon - \epsilon_0)^2 / 2\sigma^2], & \text{for } 0 \leq \epsilon \leq 1, \\ 0, & \text{otherwise,} \end{cases} \tag{3}$$

where $\mathcal{N}$ is a suitable normalization constant. If considered in the whole real domain $-\infty < \epsilon < +\infty$, this distribution has mean value ϵ_0 —that will be here restricted to the interval $0 \leq \epsilon_0 \leq 1$— and mean square dispersion σ. The case of homogeneous coupling is recovered for $\sigma = 0$. In this limit, since the Lyapunov exponent of the logistic map in eq. (2) is $\lambda = \ln 2$, full synchronization is linearly stable for $\epsilon > 1/2$.

For $\sigma \neq 0$, the coupling intensities chosen from the distribution (3) are spread around ϵ_0. From eq. (2) it is clear that full synchronization, in which $x_i(t) = x_j(t)\ \forall\ i,\ j$ and t, is a possible state for the inhomogeneous population. As in the homogeneous case, if the fully synchronized state is reached, each element follows the behaviour of a single, uncoupled mapping. It can be expected that, for each value of σ, there is a minimum critical value of ϵ_0 above which full synchronization is stable. This critical value has here been determined through numerical simulations in a population of $N = 10^4$ elements [11]. At each selected point (ϵ_0, σ), the coupled population has been left to evolve from a random initial condition and, after a maximum of 10^4 temporal steps, it has been tested whether the fully synchronized state was reached. A polynomial interpolation of the boundary of the zone where full synchronization is observed is shown as a line in fig. 1. Full syncronization occurs in the zone of small σ and large ϵ_0.

Performing a linear stability analysis of the fully synchronized state is not a simple task. It involves the diagonalization of a random matrix with strong correlations between its elements. A weaker condition for stability can however be easily stated: if the coupling intensity of at least one element i in the population is $\epsilon_i < 1/2$, full synchronization is *unstable*. A possible criterion to define the stability region in the (ϵ_0, σ)-plane is therefore the following. If the values of ϵ_0 and σ are such that the expected number of elements with $\epsilon_i < 1/2$ is greater than unity, full synchronization is unstable. Within this criterion, the boundary of the stability region is given by the identity

$$N^{-1} = \int_0^{1/2} P(\epsilon)\ \mathrm{d}\epsilon\,, \tag{4}$$

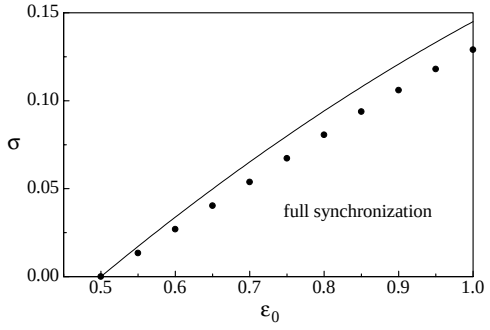

Fig. 1

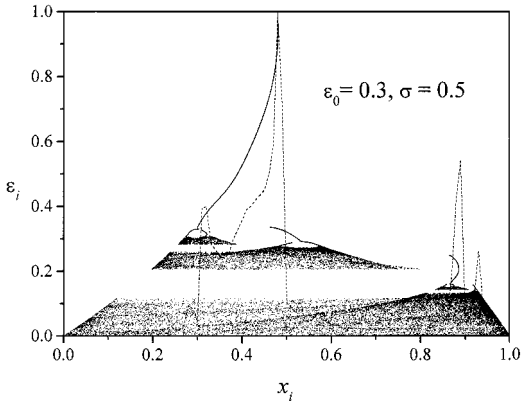

Fig. 2

Fig. 1. – The region of full synchronization in the (ϵ_0, σ)-plane, calculated from numerical simulations (full line) and from eq. (4) (dots).

Fig. 2. – Snapshot of the population in the (x_i, ϵ_i)-plane, for $\epsilon_0 = 0.3$ and $\sigma = 0.5$. The dashed line is a 100-column histogram of the projection over the horizontal axis. The histogram is normalized such that its maximum equals unity.

where $P(\epsilon)$ depends parametrically on ϵ_0 and σ. Dots in fig. 1 stand for the values of these parameters that satisfy eq. (4) for $N = 10^4$. These results show that the approximation (4) is a reasonable one. Note however that the above criterion depends on N and approaches a trivial limit for $N \to \infty$, whereas the region of full synchronization is expected to be well defined in that limit.

In a homogeneous population of coupled maps, the state of full synchronization is preceded —as the coupling intensity increases— by a regime of clustering [5, 7]. In this regime, the population is spontaneously divided into groups of elements with identical evolution. It can be seen, from eq. (2), that such kind of clustering is not possible in an inhomogeneous population. For this system, a different form of collective evolution is observed outside the region of full synchronization. The dashed line in fig. 2 shows a histogram of the distribution of 10^5 elements in the coordinate space at a given time, for $\epsilon_0 = 0.3$ and $\sigma = 0.5$. Evidently, this distribution is highly inhomogeneous, with sharp spikes of different heights at several points. Note, however, that it differs from a strictly clustered distribution, typical of homogeneous populations, where the histogram consists of several isolated peaks [7]. At each time step —as the system evolves— the histogram changes, but it preserves its strongly peaked profile. This state of partial synchronization is therefore characterized by the appearence of correlations in the form of accumulation of elements in certain regions of the coordinate space.

The underlying complexity of the partially synchronized state is fully revealed when analyzing the correlation between the coordinate x_i of each element i and the corresponding value of the coupling intensity ϵ_i. This non-trivial correlation had been preliminary reported in [10] for a uniform coupling distribution. Dots in fig. 2 show the coupling intensity of each element *vs.* its coordinate. Surprisingly enough, this plot resembles strongly the bifurcation diagram of the logistic map. A closer look, in fact, shows that it exhibits self-similar properties, although some features differ from those observed in period-doubling bifurcations. For instance, some branches are discontinuous and, around certain values of ϵ_i (as for $\epsilon_i \approx 0.22$), both disordered regions ($0.2 < x_i < 0.7$) and ordered distributions ($x_i \approx 0.85$) are observed. As in the case

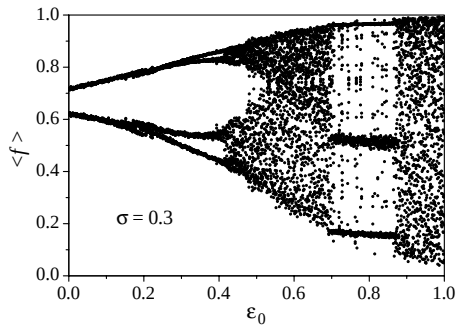

Fig. 3

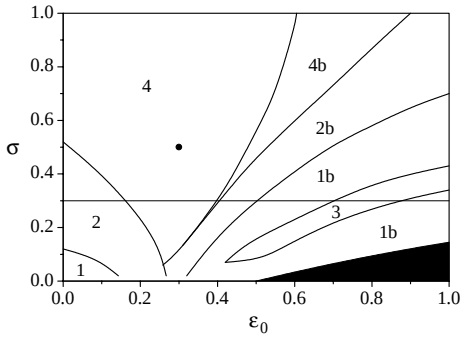

Fig. 4

Fig. 3. – Bifurcation diagram for the average $\langle f \rangle$ as a function of ϵ_0 for $\sigma = 0.3$.

Fig. 4. – Phase diagram in the (ϵ_0, σ)-plane, indicating the regions of different behaviour of $\langle f \rangle$. Zones labeled with n correspond to period-n cycles, whereas nb indicates chaotic motion in n bands. The dark zone is the region of full synchronization. The horizontal line stands for the points where the data in fig. 3 was obtained. The dot in the period-4 zone corresponds to fig. 2.

of the histogram, this distribution changes as time goes on, but its topological features are preserved during the evolution.

Self-similar features in the ϵ_i *vs.* x_i plot of fig. 2 imply a complex, hierarchical distribution of elements in the coordinate space. For large values of ϵ_i, a regular distribution is observed. Elements with similar coupling intensities are neighbours in space. When a bifurcation occurs for a given value of ϵ, the population with slightly higher coupling intensities splits into two groups, which separate from each other as ϵ_i grows. Eventually, a disordered regime is reached, where elements with similar values of ϵ occupy relatively large regions. Around a given value of x_i, regular and disordered regimes can occur simultaneously. Near $x_i = 0.35$, for instance, four clearly distinct groups are present. Three of them —with low coupling intensities— are disordered, whereas the fourth —with relatively large values of ϵ_i— is regular.

It is worthwhile to note that disordered distributions, where elements with similar ϵ_i are widely spread in the coordinate space, correspond to disordered (seemingly chaotic) evolution of the individual elements. On the other hand, as explained below, regular distributions —such as for large ϵ_i— correspond to regular (but noisy) dynamics.

In order to provide an explanation for the complex behaviour exhibited by the present system, eq. (2) can be reinterpreted as an autonomous mapping for a single element with effective dynamics $x_i(t+1) = f_{\text{eff}}[x_i(t)]$ under the action of an external additive forcing $\epsilon_i \langle f(t) \rangle$. The effective individual dynamics is given by a logistic map with a modified constant, $f_{\text{eff}}(x_i) = r_i x_i (1 - x_i)$ with $r_i = 4(1 - \epsilon_i)$. Regarding the "external" forcing, of course, its dynamics is a collective property of the ensemble and depends therefore on the state of each element. There follows a well-defined average evolution with fluctuations originated inside the system, due to the large number of degrees of freedom in the population. From a phenomenological point of view, however, it enters the individual dynamics as an independent term, whose average evolution and fluctuations can be considered to be fixed from outside the single-element system. Within this picture, thus, the evolution of a single element results from the combined effect of the effective individual dynamics —which has the well-known logistic behaviour— and the external noisy forcing. It is therefore necessary to characterize now the dynamics of the external forcing and, in particular, of the average $\langle f(t) \rangle$.

Figure 3 shows the bifurcation diagram of $\langle f \rangle$ as a function of ϵ_0, for $\sigma = 0.3$ and $N = 10^4$. It has been constructed by letting the system evolve, for each value of ϵ_0, during a transient of 10^3 time steps and then recording the next 10 values of $\langle f \rangle$. At the end of this transient, both the average evolution and the internal noise have already attained a stationary regime. The step length in ϵ_0 is $\Delta\epsilon_0 = 3 \times 10^{-3}$. For $\epsilon_0 = 0$, $\langle f(t) \rangle$ is engaged in a cycle of period 2, with moderate fluctuations generated as explained above. For $\epsilon_0 \approx 0.2$ the cycle bifurcates to a period-4 orbit. Note that this bifurcation differs qualitatively from those observed in the logistic map. This suggests that the evolution of $\langle f \rangle$ does not belong to the universality class of quadratic mappings. Higher-order bifurcations are suppresed by noise. For larger ϵ_0, thus, the bifurcation diagram shows a chaotic zone with four bands which merge into two bands and, eventually, into a single band for $\epsilon_0 \approx 0.5$. This regime persists up to $\epsilon_0 = 1$, except for a wide stability window ($0.7 \lesssim \epsilon_0 \lesssim 0.87$), where $\langle f \rangle$ displays a noisy cycle of period 3.

The kind of bifurcation diagrams exhibited by $\langle f \rangle$ as a function of ϵ_0 for other values of σ is similar to that of fig. 3. Typically, a cascade of noisy bifurcations leads to a chaotic zone where a period-3 window may appear. All these bifurcations are of the same type as shown in fig. 3 for $\epsilon_0 \approx 0.2$, namely, they do not show the characteristic pitchfork shape of bifurcations in quadratic maps. Figure 4 shows an approximate phase diagram for the behaviour of $\langle f \rangle$, extracted from simulations of an ensemble of 10^4 elements. In the zones marked with the label n, $\langle f \rangle$ evolves in a noisy cycle of period n, whereas in the zones marked with nb it evolves in chaotic orbits that visit n bands alternately. The boundaries between zones have been approximated by polynomial fitting of the numerical data. These show considerable dispersion, especially, in the boundaries separating regular and chaotic evolution, where noise suppresses the intermediate bifurcations. The dark region in fig. 4 is the zone of full synchronization, which —since the synchronized population is driven by the logistic map in the extreme chaotic limit— corresponds to chaotic evolution in a single band. Note the wide period-3 window immersed in the 1b zone. The horizontal line in this plot stands for the points where the bifurcation diagram of fig. 3 was calculated, whereas the dot in the region of period 4 corresponds to the parameters of fig. 2.

The phase diagram of fig. 4 shows that, for the parameter set of fig. 2, $\langle f(t) \rangle$ in engaged in a period-4 orbit. In order to reobtain fig. 2 in the frame of the single-element picture proposed above, the temporal average $\overline{\langle f \rangle}$ and the mean dispersion $\delta\langle f \rangle$ of each one of the four successive values of $\langle f(t) \rangle$ have been measured. Then, a single element with the logistic dynamics given by f_{eff}, subject to a noisy period-4 external forcing constructed with those measured parameters, has been left to evolve from a randomly chosen initial condition. For different values of ϵ_i and appropriately choosing the time at which the state of the element is measured —namely, always with the same phase with respect to the periodic forcing— fig. 2 is in fact accurately reproduced. This supports applying the dynamical representation of an individual element in the coupled population as an effective map driven by an external force. Within this picture, a phenomenon such as the coexistence of regular and chaotic motion for a given value of the coupling intensity ϵ_i —as observed in fig. 2 near $\epsilon_i = 0.22$— can be readily explained. In fact, the possibility of obtaining both types of motion from different initial conditions at fixed values of the parameters that control the evolution is a well-known property of dynamical systems subject to periodic forcing [12].

It should be expected that certain details in the phase diagram of fig. 4 depend on the number of elements in the population. Indeed, as mentioned above, the suppression of higher-order periodic motion in $\langle f(t) \rangle$ —as well as the absence of higher-order periodicity windows in the chaotic region— are to be ascribed to the noise generated by the population itself. This results in random-like fluctuations in $\langle f \rangle$, that could be supposed to self-average as the number N of elements in the population grows. It has been however shown [13] that,

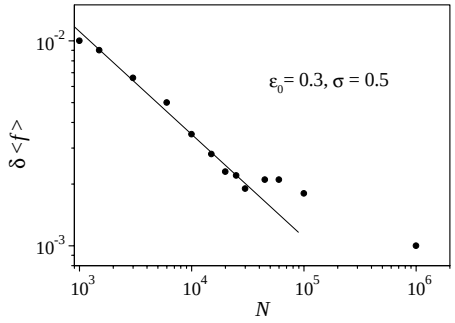

Fig. 5. – Size dependence of the fluctuations in $\langle f \rangle$ for $\epsilon_0 = 0.3$ and $\sigma = 0.5$. The straight line in this log-log plot has slope $-1/2$.

in large populations of globally coupled identical dynamical elements, self-averaging does not occur at the same rate as in ensembles of independent elements. Namely, the law of large numbers, $\delta\langle f \rangle \sim N^{-1/2}$, breaks down in globally coupled populations. Fluctuations in ensemble averages show in fact a much slower decrease as N grows. This remarkable feature has been interpreted as an emerging property in the collective evolution of the population, with origin in the long-range interactions between its components [13, 14].

To test this property in eq. (2), the fluctuations $\delta\langle f \rangle$ have been measured for the largest of the four values that $\langle f(t) \rangle$ visits in its period-4 cycle at $\epsilon_0 = 0.3$ and $\sigma = 0.5$. Results are shown in fig. 5. In this plot, two regimes are clearly identified. For $N \lesssim 3 \times 10^4$, the law of large numbers, $\delta\langle f \rangle \sim N^{-1/2}$, does hold. In the log-log plot of fig. 5, this has been emphasized by drawing a straight line with slope $-1/2$ in the low-N range. Above this range, it is apparent that the law of large numbers breaks down, and the fluctuations in $\langle f \rangle$ vary more slowly with N. The presence of a relatively wide range where the law of large numbers holds can be ascribed, in the present system, to an inherent random ingredient in the population, namely, the values of the coupling intensities ϵ_i. This stochastic component seems to dominate the fluctuations of the average $\langle f \rangle$ for small N. Since there is no correlation between the values of ϵ_i for different elements, the effect of their random distribution verifies the law of large numbers and self-averages then in the usual way. At a certain point, however, it becomes less important than the fluctuations originated in the dynamics itself, which —as explained above— are expected to vary with N in a relatively slow manner. This variation thus dominates in the large-N regime.

In summary, it has been here shown that a population of globally coupled logistic maps where the effect of coupling is heterogeneous, *i.e.*, where each element has a different coupling intensity, can perform fully synchronous motion —as observed in homogeneous populations— when coupling intensities are distributed with large mean value and relatively small dispersion. On the other hand, clustering is not possible here. Synchronization is instead replaced by a regime where the elements display a complex dynamical distribution in the coordinate space, exhibiting a highly non-trivial correlation with their coupling intensities. This correlation, which had already been preliminary reported for coupled logistic maps with a uniform coupling distribution [10], is probably a distinctive feature of inhomogeneous populations of globally coupled dynamical systems. In this sense, it would be interesting to detect its occurrence in ensembles where the dynamical elements differ from each other and are globally coupled in a homogeneous way [1, 7, 8].

The observed correlation between the spatial distribution and the coupling intensities can be explained by interpreting the dynamics of each element as the combined effect of an effective autonomous evolution and an "external" fluctuating force, which is actually generated inside the system. The dynamics of this "external" force also displays complex features, such as bifurcations and chaos, to which the internal noise originated in the population is superposed. For small populations, these fluctuations self-average as predicted by the law of large numbers —presumably due to the dominant effect of the random distribution of coupling intensities. This has also been observed in globally coupled ensembles with slightly different elements or subject to external noise [15]. For large populations, instead, emerging collective properties in the dynamics make that law break down and fluctuations result to be more persistent as the number of elements grows. It could be expected that at least a part of the features summarized above are generically found in populations of dynamical elements —different from logistic maps— when coupling is inhomogeneous. This is the subject of work in progress.

***

Financial support from Fundación Antorchas, Argentina, is gratefully acknowledged.

REFERENCES

[1] Kuramoto Y., *Chemical Oscillations, Waves and Turbulence* (Springer, Berlin) 1984.
[2] Khrustova N., Veser G., Mikhailov A. and Imbihl R., *Phys. Rev. Lett.*, **75** (1995) 3564.
[3] Abarbanel H. D. *et al.*, *Phys. Usp.*, **39** (1996) 337; Sompolinsky H., Golomb D. and Kleinfeld D., *Phys. Rev. A*, **45** (1991) 6990.
[4] Winfree A. T., *The Geometry of Biological Time* (Springer, Berlin) 1980.
[5] Kaneko K., *Physica D*, **23** (1986) 436; **37** (1989) 60; **54** (1991) 5.
[6] Kaneko K., *Physica D*, **41** (1990) 137.
[7] Zanette D. H. and Mikhailov A. S., *Phys. Rev. E*, **57** (1998) 276.
[8] Pikovsky A. S., Rosemblum M. G. and Kurths J., *Europhys. Lett.*, **34** (1996) 165.
[9] Zanette D. H., *Phys. Rev. E*, **55** (1997) 5315.
[10] Kaneko K., *Physica D*, **75** (1994) 55.
[11] To avoid spurious round-off effects in the simulations, the map in eq. (2) is taken to be $f(x) = rx(1-x)$ with $r = 4 - \delta$ and $\delta = 10^{-4}$. Its dynamical properties are essentially the same as for $r = 4$.
[12] Moon F. C., *Chaotic Vibrations* (John Wiley, New York) 1987.
[13] Kaneko K., *Phys. Rev. Lett.*, **65** (1990) 1391.
[14] Perez G., Sinha S. and Cerdeira H. A., *Physica D*, **63** (1993) 341.
[15] Kaneko K., *Physica D*, **55** (1992) 368; Shibata T. and Kaneko K., *Europhys. Lett.*, **38** (1997) 417.